American Mineralogist, Volume 85, pages 354–363, 2000

Constraints on the *P-V-T* equation of state of $MgSiO_3$ perovskite

SANG-HEON SHIM* AND THOMAS S. DUFFY

Department of Geosciences, Princeton University, Princeton, New Jersey, 08544, U.S.A.

ABSTRACT

Equation of state fits to experimental *P,V,T* data were examined by the inversion of synthetic data sets using the thermoelastic parameters of $MgSiO_3$ perovskite. Our results show that by extending the pressure and temperature range to 130 GPa and 2500 K, the volume dependence of the Grüneisen parameter, q ($=\partial\ln\gamma/\partial\ln V$), could be resolved to ~10% under the best circumstances. However, simulations also showed strong correlation between the bulk modulus, K_{T0}, and its pressure derivative, K'_{T0}, and q within the currently accepted uncertainty of elastic parameters for $MgSiO_3$ perovskite. We considered the effect of random error based on the reported uncertainty for different measurement techniques. Even though the laser heated diamond-anvil cell (LHDAC) technique has significantly larger temperature uncertainty, the ability to extend the pressure and temperature ranges allows for improved resolution of higher order thermodynamic parameters. However, systematic error from temperature inhomogeneity in the LHDAC sample could result in overestimation of q. We also performed Birch-Murhanghan-Debye (BMD) equation of state (EOS) fits for currently available data sets. Consistent with the simulation results, combining recent LHDAC (Fiquet et al. 1998) and resistance heated diamond-anvil cell (RHDAC) (Saxena et al. 1999) with lower *P-T* measurements (Ross and Hazen 1989; Wang et al. 1994; Utsumi et al. 1995; Funamori et al. 1996) we obtained q = 2.0(3) and γ_0 = 1.42(4). The difference between q = 2.0(3) and the normally assumed value of q =1 strongly affects calculated values for higher order thermoelastic parameters [e.g., α, $(\partial K_T/\partial T)_P$] as well as first order parameters, such as density and bulk modulus at lower mantle conditions. However, possible systematic error sources need to be further investigated and measurements at higher *P-T* conditions promise to yield better constraints on the thermoelastic parameters of $MgSiO_3$ perovskite.

INTRODUCTION

The lower mantle plays an important role in understanding the dynamics and evolution of the Earth. However, fundamental questions about this region remain unanswered. Recent studies have uncovered new evidence of chemical stratification or heterogeneity in the deep lower mantle (Kellogg et al. 1999; van der Hilst and Kárason 1999). Tomographic images appear to show subducting slabs penetrating into the lower mantle (van der Hilst et al. 1997), but the ultimate fate of these slabs is uncertain (Kesson et al. 1998; Hirose et al. 1999). The D" region at the base of the mantle has been shown to be a region of complex seismic behavior the origin of which is not well understood (Williams et al. 1998).

Due to the lack of direct samples from the lower mantle, seismic observations and laboratory measurements are the only available means to understanding this region. $MgSiO_3$ perovskite is believed to be the major constituent of the Earth's lower mantle (Liu 1976; Knittle and Jeanloz 1987; Tomioka and Fujino 1997). Thus, the physical and chemical properties of this material are crucial to understanding those of the lower mantle.

The *P-V-T* equation of state (EOS) plays a central role in study of the Earth's deep interior. Using the EOS, we can calculate the densities and bulk wave velocities of candidate materials at lower mantle *P, T* conditions. By fitting the densities and wave velocities to seismic observations, one can test models for the bulk chemistry of the lower mantle (e.g., Stixrude et al. 1992; Wang et al. 1994; Hemley et al. 1992; Bina 1995; Jackson 1998). In addition, the EOS enables us to determine the depth dependence of important thermoelastic parameters such as thermal expansivity and temperature sensitivity of the bulk modulus. The latter is necessary for comparing seismic bulk velocity profiles to laboratory data. The importance of the pressure dependence of thermal expansivity for planetary interiors was recognized early on by O. L. Anderson (1967). Recent work by Anderson and colleagues has provided important insights into thermal expansivity in general, and the thermodynamic properties of $MgSiO_3$ perovskite in particular (e.g., Anderson et al. 1990; Anderson and Masuda 1994; Anderson et al. 1995; Anderson 1998).

The *P-V-T* EOS is obtained by fitting experimentally measured volumes at various *P-T* conditions. Static *P-V-T* EOS data have been reported using different types of experimental apparatus which cover different *P-T* ranges and have different experimental precision. For the large volume press (LVP), typical uncertainties are ~2–4% for pressure, ~0.1% for volume, and ~1% for temperature (Wang et al. 1994; Funamori et al. 1996). Recently, new methods using the diamond cell combined with laser or resistance heating have been used to obtain *P-V-T* EOS

*E-mail: sangshim@princeton.edu

data directly at lower mantle *P-T* conditions (Fiquet et al. 1998; Shim et al. 1998; Shen and Rivers 1998; Saxena et al. 1999). It can be expected that extension of data coverage to a pressure more than a factor of two larger using these techniques could improve the precision and accuracy of fitted parameters. However, compared with the LVP, laser heated diamond-anvil cell (LHDAC) data have much larger uncertainty (order of magnitude) for temperature.

Extensive discussion of the merits of various alternative forms of the *P-V-T* EOS for fitting experimental data is contained in Jackson and Rigden (1996). In their study, model and real data sets were used to explore both the EOS formulation and best fitting thermoelastic parameters obtainable from existing data sets for β-$(Mg,Fe)_2SiO_4$ and $MgSiO_3$ perovskite. These data sets, which were obtained using the resistively heated diamond anvil cell (Fei et al. 1992) and the LVP (Wang et al. 1994; Utsumi et al. 1995; Funamori et al. 1996), extend to a maximum pressure of 29 GPa. Here we use similar methods as Jackson and Rigden (1996) to explore the constraints on thermoelastic parameters that we can expect to obtain using the new diamond cell techniques that can reach pressure of 100 GPa or more.

In this study, we examine the confidence range of the estimated parameters by fitting to synthetic data sets which are generated to simulate data from the different experimental techniques. This method also enables us to study the correlation between fitted parameters and the effect from different error sources. In addition, based on these results, we will show results for currently available *P-V-T* measurements on $MgSiO_3$ perovskite and discuss the limitations and problems of these data sets. Finally, we will propose optimal conditions for future measurements to improve the resolution of the fitted parameters of the *P-V-T* EOS of $MgSiO_3$ perovskite.

P-V-T EQUATION OF STATE

In the Mie-Grüneisen approach, the total pressure, $P_{tot}(V,T)$, can be expressed as a sum of the static pressure, P_{st}, i.e., isothermal compression at 300 K, and the thermal pressure increases along an isochore, ΔP_{th}:

$$P_{tot}(V,T) = P_{st}(V) + \Delta P_{th}(V,T). \quad (1)$$

The third-order Birch-Murnaghan equation has been widely used to describe isothermal compression of mantle minerals:

$$P_{st} = \frac{3}{2}K_{T0}\left[\left(\frac{V_0}{V}\right)^{7/3} - \left(\frac{V_0}{V}\right)^{5/3}\right]\left\{1 - \frac{3}{4}(4 - K'_{T0})\left[\left(\frac{V_0}{V}\right)^{2/3} - 1\right]\right\}, \quad (2)$$

where K_{T0} is the isothermal bulk modulus, K'_{T0} is the pressure derivative of the bulk modulus, and V_0 the volume. The subscript 0 refers to ambient conditions (1 bar and 300 K).

The thermal pressure can be described using the Debye model (Jackson and Rigden 1996):

$$\Delta P_{th} = \frac{\gamma(V)}{V}\left[E_{th}(V,T) - E_{th}(V,T_0)\right], \quad (3)$$

$$E_{th} = \frac{9nRT}{(\theta/T)^3}\int_0^{\theta/T}\frac{\xi^3 d\xi}{e^{\xi}-1} \quad (4)$$

$$\gamma = \gamma_0\left(\frac{V}{V_0}\right)^q \quad (5)$$

$$\theta = \theta_0 \exp\left(\frac{\gamma_0 - \gamma(V)}{q}\right). \quad (6)$$

E_{th} is the vibrational energy for a given volume and temperature, R is the gas constant, γ is the Grüneisen parameter, q is the volume dependence of the Grüneisen parameter (q = dlnγ/dln$V$) which is assumed to be constant, n is the number of atoms per formula unit, and θ is the Debye temperature.

Figure 1 shows example isotherms and thermal pressures calculated using the Birch-Murhanghan-Debye (BMD) equation for the thermoelastic parameters of $MgSiO_3$ perovskite (Table 1). In the *P-V* plane, the thermal pressure term is given by the spacing between isotherms at a given volume. As shown in Equations 3–6, all the volume dependences are expressed as functions of q. Thus, the variation of thermal pressure with volume determines q during EOS fitting (Fig. 1b).

The Debye approach (Eq. 3) provides a description of thermal pressure without the truncation problem that can arise when one uses a polynomial expansion (Jackson and Rigden 1996). This enables determination of thermoelastic parameters and their pressure and/or temperature dependence in an internally consistent fashion. Furthermore, Anderson (1998) demonstrated that high *P-T* behavior of $MgSiO_3$ perovskite can be well described by the Debye model by determining specific heat, entropy, and thermal pressure using the Debye model and comparing with experimental data.

FITTING TO SYNTHETIC *P-V-T* DATA SETS

To test the reliability and sensitivity of the BMD equation fit, we created several synthetic data sets that reflect varying experimental conditions, such as pressure range, temperature range, amount of random error and systematic error on *P,V,T* data in order to simulate data from various experimental techniques. *P,T* points were generated randomly within a given pressure and temperature range. This situation is similar to that of the LHDAC. Isothermal measurement conditions, such as are often found with LVP data, were also simulated by fixing the temperature range and temperature increment, and then generating pressure randomly. From these *P,T* points, the volumes were calculated using the BMD equation with thermoelastic parameters (Table 1) for $MgSiO_3$ perovskite that agree with those proposed by Jackson and Rigden (1996).

Error-free data sets were first used to investigate the effect from the pressure and temperature range of the data, and correlation between parameters. Subsequently, each data point was perturbed by noise in order to simulate the effect of random error. The amount of random error were determined based on the published precision of each technique (Table 2). The noise was calculated using a Gaussian random number generation routine (Press et al. 1988) by assigning 1σ as the value given in Table 2. Systematic temperature errors were simulated by shifting the temperature values by a prescribed amount, in addition to the random error applied to these points.

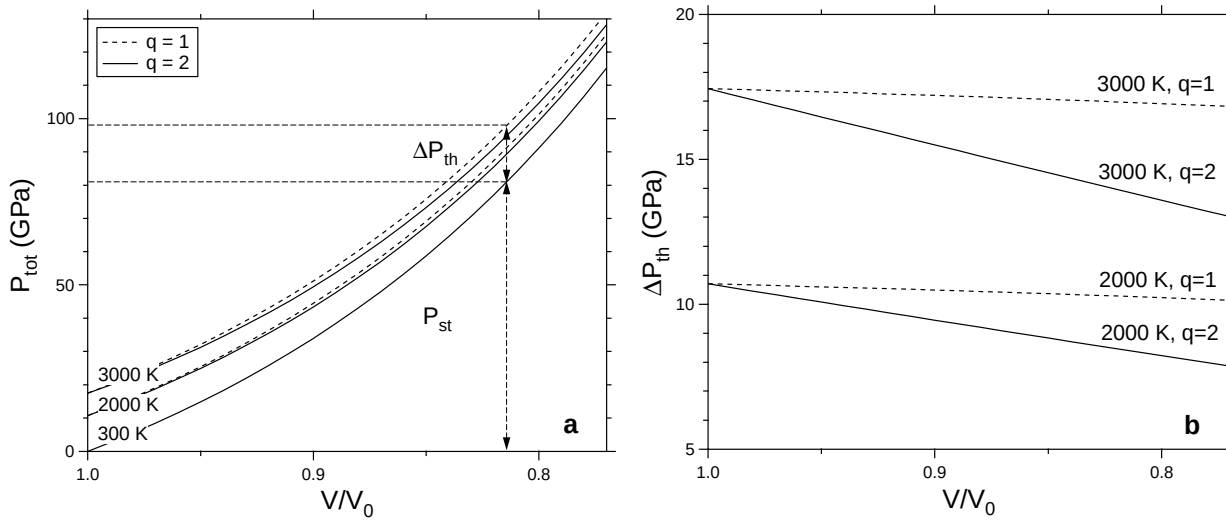

FIGURE 1. The (**a**) isotherms and (**b**) thermal pressure calculated using the BMD equation with the thermoelastic parameters of $MgSiO_3$ perovskite (Table 1) vs. normalized volume. To illustrate the effect of variations in q, we calculated isotherms for $q = 2$ (solid lines) and $q = 1$ (dashed lines).

TABLE 1. Thermoelastic parameters used to create synthetic data sets for $MgSiO_3$ perovskite

Parameter		Reference
V_0 (Å^3)	162.3	Ross and Hazen (1989)
K_{T0} (GPa)	261	Mao et al. (1991)
K'_{T0}	4	Mao et al. (1991)
γ_0	1.33	Jackson and Rigden (1996)
q	1	assumed
θ_0 (K)	1000	Jackson and Rigden (1996)

TABLE 2. Pressure-temperature range and standard deviations (1σ) assumed for P, V, and T measurement for each experimental technique

Techniques	P (GPa)	T (K)	$\sigma(P)$ (GPa)	$\sigma(T)$ (K)	$\sigma(V)$ (Å^3)
LVP	0–30	300–2000	0.5	10	0.2
LHDAC	0–130	300,1500–3000	1.0	50,100,200	0.2
RHDAC	0–70	300–1500	1.0	20	0.2

Notes LVP = Large volume press; LHDAC = Laser-heated diamond anvil cell; RHDAC = Resistivity-heated diamond anvil cell.

A non-linear least square fit routine using the Levenberg-Marquardt method (Press et al. 1988) was used to fit the data to the BMD equation. This enables us to fit all the parameters in BMD equation (V_0, K_{T0}, K'_{T0}, γ_0, q, θ_0). No weighting was used for the inversion of synthetic data sets. The 1σ uncertainties of the parameters were estimated from the diagonal terms of the covariance matrix during the final step of the iteration.

P-V-T EOS FITS FOR SYNTHETIC DATA SETS

To determine the precision with which thermoelastic parameters can be determined, we first constructed noise-free data sets using data of Table 1 and random *P,V,T* points covering variable pressure ranges. This synthetic data set was then inverted to obtain all six thermoelastic parameters simultaneously. The precision (1σ standard deviation) of the determination of K_{T0}, K'_{T0}, and q is greatly improved as the pressure range increases for a given number of data points (Fig. 2a). In contrast, increase of pressure range does not significantly improve the precisions of γ_0, V_0, and θ_0 (Fig. 2b).

The same type of simulations were performed for variable temperature ranges at a fixed pressure range (Fig. 3). Only the parameters related to thermal pressure (γ_0, q, and θ_0) are affected by the change of temperature range. For a fixed number of data points, an increase in temperature range from 300–1000 K to 300–3000 K greatly improves the precision of both q and γ_0 determination. These results show that a wide range of pressure and temperature is desirable to obtain the best constraints on q. As shown in Figures 2 and 3, q can be constrained to a precision of ~10% in the best case of a large *P-T* range and large number of data points.

Some of parameters of the BMD equation may also be obtained by other techniques. For example, K_{T0} and K'_{T0} can be determined by 300 K isothermal compression experiments or high-pressure ultrasonic or Brillouin scattering measurements. Because $MgSiO_3$ perovskite can be quenched, one can accurately determine V_0 by X-ray diffraction (XRD). θ_0 can be estimated from calorimetry or elastic properties. Parameters obtained from other techniques can then be fixed during data fitting. However, if the fixed value is not correct, this would result in systematic error for the fitted parameters. This is significant in the case where there is strong correlation between parameters.

To investigate this phenomenon, K_{T0} was perturbed from the value used to calculate the synthetic data by 5 GPa. The value for K_{T0} (=261 GPa) was taken from static compression measurements using a Ne pressure medium to 30 GPa (Mao et al. 1991). Their estimated uncertainty (1σ) on K_{T0} is ±4 GPa. Knittle and Jeanloz (1987) obtained $K_{T0} = 266 \pm 6$ GPa by static compression to 127 GPa without a pressure medium. K_{S0} was determined to be 264 ± 5 GPa by Brillouin scattering measurement (Yeganeh-Haeri 1994). Thus, we use ±5 GPa as the estimated uncertainty on K_{T0} based on currently available data.

Data inversions were conducted by fixing K_{T0} at 256, 261,

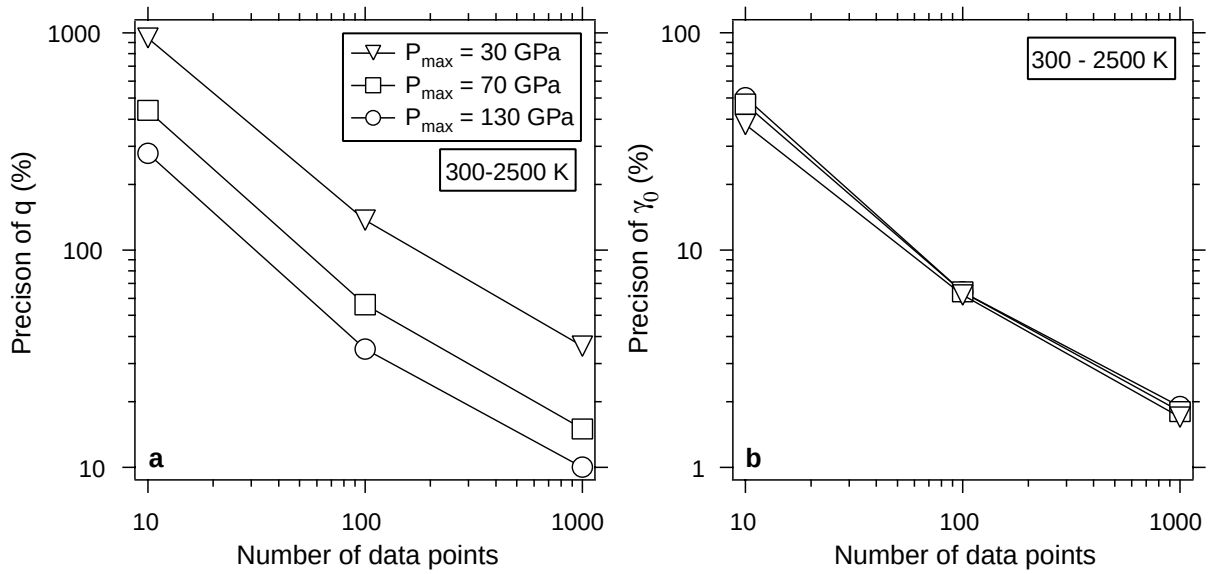

FIGURE 2. The estimated precisions (1σ) of (**a**) q and (**b**) γ_0 by synthetic data inversion vs. number of data points for variable pressure ranges of 0–30 GPa, 0–70 GPa, and 0–130 GPa, at a fixed temperature range of 300–2500 K.

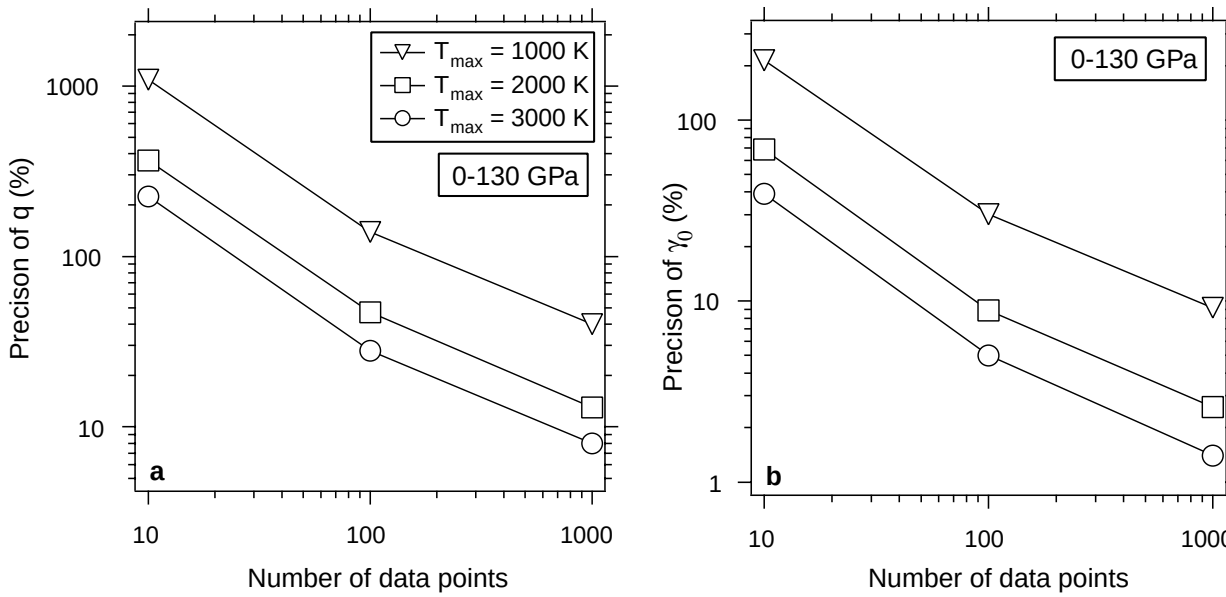

FIGURE 3. The estimated precisions (1σ) of (**a**) q and (**b**) γ_0 by synthetic data inversion vs. number of data points for variable temperature ranges of 300–1000 K, 300–2000 K, and 300–3000 K, at a fixed pressure range of 0–130 GPa.

264, and 266 GPa while other parameters were held at model values (Table 1) except for q or γ_0. The resultant value of q shows a strong correlation with K_{T0} (Fig. 4). However, γ_0 shows only weak correlation with K_{T0} (±3% variation). The strong correlation with q is also found for pressure derivative of the bulk modulus, K'_{T0}. In this case, a 10% variation of K'_{T0} yields a 60% change of q. These results emphasize the importance of reducing the uncertainity in the reference compression curve for determination of q without systematic bias. The strong sensitivity of q to the elastic parameters, K_{T0} and K'_{T0}, is related to the fact that, at high pressure, ΔP_{th} is small relative to P_{st}. When fitting 300 K *P-V* data to a Birch-Murnaghan equation, there can be tradeoffs between the fit values of K_{T0} and K'_{T0}. These tradeoffs will not affect the value of q as long as the choice of K_{T0} and K'_{T0} accurately describes the hydrostatic *P-V* curve.

Our simulation shows that θ_0 is not well resolved by the *P-V-T* EOS fit compared to other parameters in agreement with earlier studies (Hemley et al. 1992; Bina 1995; Jackson and Rigden 1996). The best approach is to fix this parameter during the fit using measurements from other techniques. For

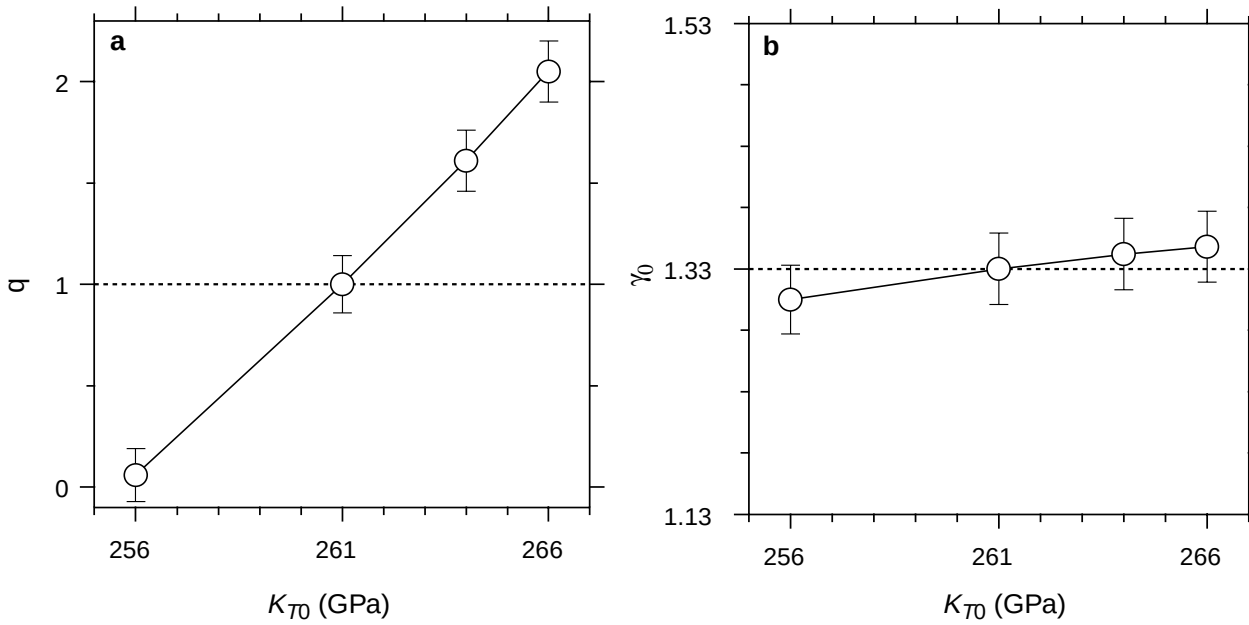

FIGURE 4. The fitted values of (**a**) q and (**b**) γ_0 vs. perturbed K_{T0} values. The synthetic data was generated for 0–130 GPa and 300–2500 K. The values used to generate synthetic data were indicated as dashed lines. The error bars are the 1σ of estimated parameters.

$MgSiO_3$ perovskite, θ_0 has been determined to be 980 ± 15 K from calorimetry data at 140–295 K (Akaogi and Ito 1993). Inversions for q and γ_0 for θ_0 values that range up to 500 K away from model values show that q and γ_0 are not strongly sensitive to an incorrect choice of θ_0. The variations of q and γ_0 are ±20% and ±8% respectively for θ_0 values ±500 K from the model value of 1000 K for synthetic data covering 0–130 GPa and 300–2500 K.

In LVP and resistance heated diamond-anvil cell (RHDAC) experiments, one can control the temperature accurately. Thus, *P,T* data points can be measured along an isotherm. However, in LHDAC experiments, it is difficult to set the temperature to a desired value during the measurement. In addition, the pressure may change during heating. In most such experiments, one obtains randomly distributed *P,T* data points. We created data which simulated both a random *P,T* distribution and isothermal conditions. The fitting results for these data sets did not show any significant difference with regard to the accuracy and the precision of fitted parameters. Therefore, we restrict our attention to the random *P,T* case throughout this paper.

To test the effect of differing uncertainties resulting from different experimental techniques, we first synthesized a data set which covers a similar data range (0–30 GPa) and has similar experimental uncertainty to the currently available LVP data set (Table 2). We created three individual data sets which have the same pressure and temperature range, errors on *P,V,T*, and distribution of data points in the *P-T* plane as those of Wang et al. (1994), Utsumi et al. (1995), and Funamori et al. (1996). The total number of data points is 250. Data sets were also created that simulate the LHDAC case by varying pressure range (30–70 GPa and 30–130 GPa) and random temperature error (50, 100, and 200 K) (Table 2). The number of data points is 50. These data sets were then combined with the LVP data set.

Due to the addition of random errors on the data points, the fitting results are affected by the scatter of the data points. We therefore generated 100 data sets and performed fits for each one. We then take an average of those results to remove the effect of individual scatter in a data set. This process also enables us to obtain the distribution of fitted parameters around the true value. This can be compared with the estimated standard deviation of fitted parameters from the covariance matrix. K_{T0}, K'_{T0}, V_0, and θ_0 were fixed throughout these calculations. No weights were used during the fitting.

As shown in Figure 5a, the scatter of fitted q values is greatly reduced by combining LHDAC data and LVP data. Moreover, even when we have more than one order of magnitude higher errors on temperature for the LHDAC data (200 K), by expanding the pressure range (to 130 GPa in this case), the scatter of the resulting q value is lower than obtained from the LVP data alone. In contrast, γ_0 is not improved significantly by combining LHDAC with LVP data. The scatter of γ_0 is also not sensitive to the effect of the relatively large temperature error of the LHDAC data. The thermal pressure term is relatively more important in the lower pressure and high-temperature region which is covered in LVP experiments ($P \leq 30$ GPa and $T \leq$ 2000 K) (Funamori et al. 1996). However, as pressure increases, even at very high temperature, the contribution of the thermal term to the total pressure decreases to less than 10%. γ_0, which is the main contribution to the thermal pressure term, is thus mainly controlled by low pressure but high-temperature data points. Although q is also part of the thermal pressure term, since q is the volume dependence of γ_0, a large

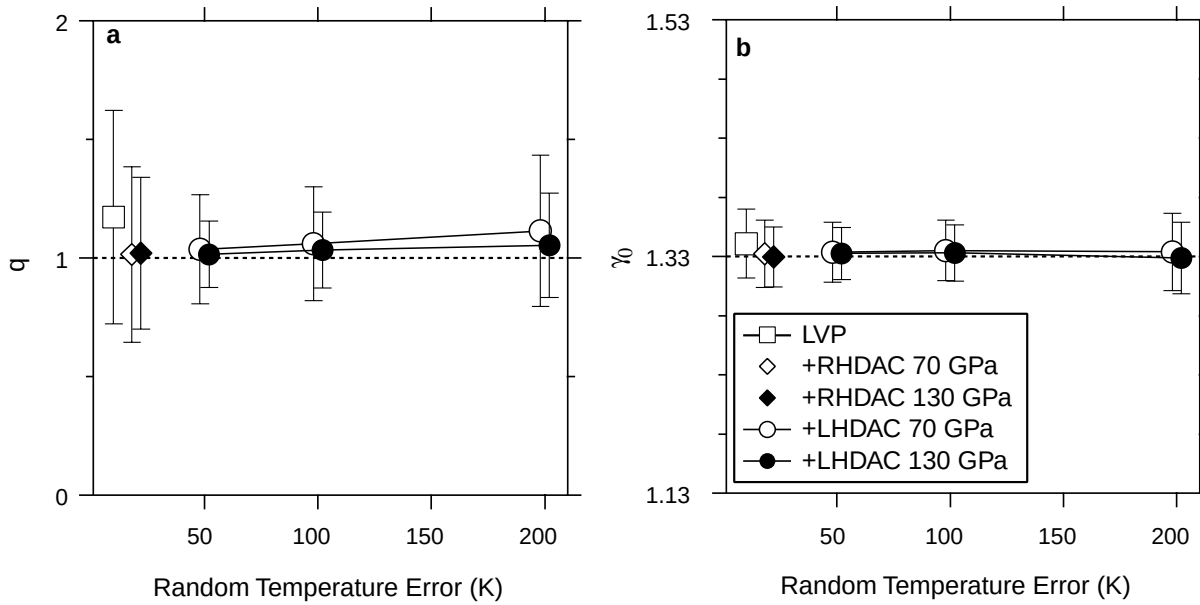

FIGURE 5. The fitted values of (**a**) q and (**b**) γ_0 vs. the random temperature error (1σ). The synthetic data covered a pressure range of 0–70 GPa and 0–130 GPa. The values used to generate synthetic data are indicated as dashed lines. The symbols represent the average of fitted parameters and the error bars are the standard deviation (1σ) from inversions of 100 data sets. The points are slightly shifted from each other to prevent overlap of symbols.

variation in volume is needed to determine q reliably. Therefore, the larger *P-T* range improves the resolution of this parameter. The LHDAC technique can readily achieve this condition, despite the larger uncertainty in temperature.

The RHDAC data sets were synthesized in similar manner as for LHDAC. However, the error and range of temperature are less than that of LHDAC. Figure 5 shows that RHDAC data also improves the resolution of q. However, because of its limited temperature range (in this study we assume that it is limited to below 1500 K), the standard deviation of q is bigger than that of LHDAC measurement. Compared to LVP data alone, the larger pressure range of the RHDAC provides a clear advantage.

One final point regarding Figure 5 is that the estimated uncertainties of the fitted parameters from the covariance matrix agree with the standard deviation determined directly by fitting to 100 data sets. For example, the estimated error range of γ_0 is ±0.02 and q is ±0.2 for pressure range of 30–130 GPa and random noise of temperature 100 K. This agrees well with the data point shown in Figure 5. This means that despite the lack of weights for data from different techniques, the estimated error range using the least-square routine appears realistic. However, this result is based on the assumption that we only have random errors for *P,V,T*.

There are many possible sources of systematic error for high *P-T* experiments, such as the *P-V-T* EOS of the internal standard, non-hydrostatic stresses in the sample, misalignment of XRD system, inhomogeneous heating, and so on. One of the most serious problems for LHDAC measurements are radial and axial temperature gradient in the sample. By decreasing the X-ray beam size and increasing the laser beam diameter, the thermal gradients are reduced in the radial direction (Shen and Rivers 1998). To decrease the axial gradient, the sample thickness may be decreased but this reduces the quality of the XRD pattern. Recently a new laser heating system has been developed at the Advanced Photon Source using double sided laser heating (Shen and Rivers 1998) (Fig. 6). By measuring temperatures from both sides of a sample heated from one side only, Shen and Rivers (1998) found a greater than 200 K thermal gradient along the axial direction.

To simulate the effect of this systematic error on the fitted parameters, we tested a simple case. For a single-sided heating system, we assume that laser heats a finite depth of the sample (Fig. 6a). This is appropriate for the case of a non-absorbing sample (e.g., $MgSiO_3$ perovskite) mixed with an absorbing medium (e.g., platinum). In this case, the volume measured by X-ray diffraction is an average along the axial temperature gradient. However, most of the thermal radiation will come from the surface where the sample is hottest. Therefore, the measured temperature by radiometry will be higher than the average temperature sampled by the X-ray beam. As a result, the temperature will be systematically overestimated. This situation can be simulated by adding systematic errors to the data. In this case, we perturb each temperature by a fixed amount (50, 100, and 200 K) and then add random error as was done previously. Again, 100 data sets were inverted.

As shown in Figure 7, systematic overestimation of temperature results in q being significantly overestimated. This effect is less pronounced for the larger pressure range. γ_0 is relatively insensitive to the systematic temperature error of LHDAC data. Interestingly as pressure range increases, underestimation of γ_0 becomes more significant (Fig. 7b). This may be due to the correlation between q and γ_0 during fitting; the

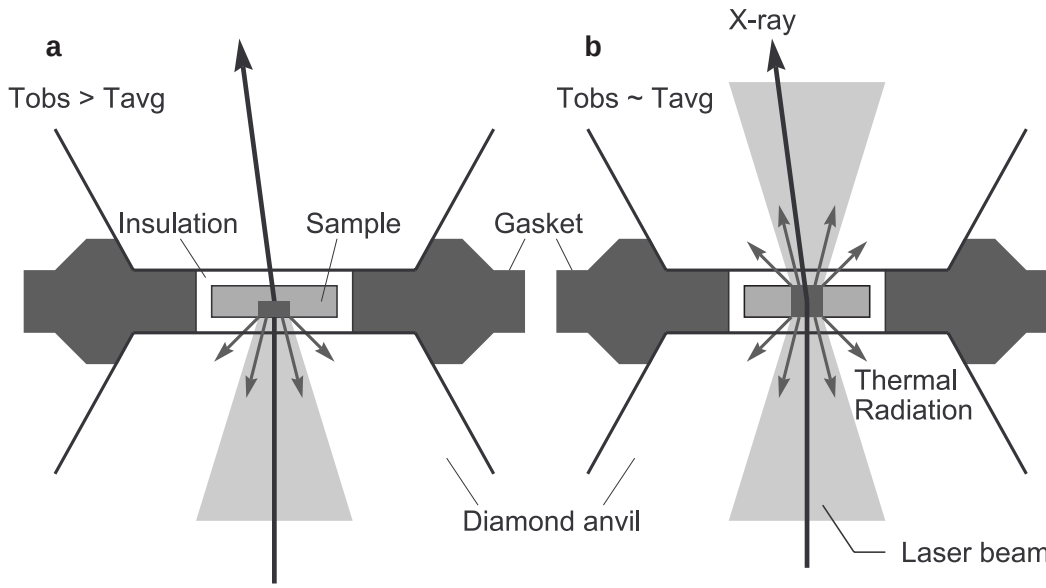

FIGURE 6. Schematic diagram of laser heated diamond-anvil cell with (**a**) single-sided heating geometry and (**b**) double-sided heating geometry.

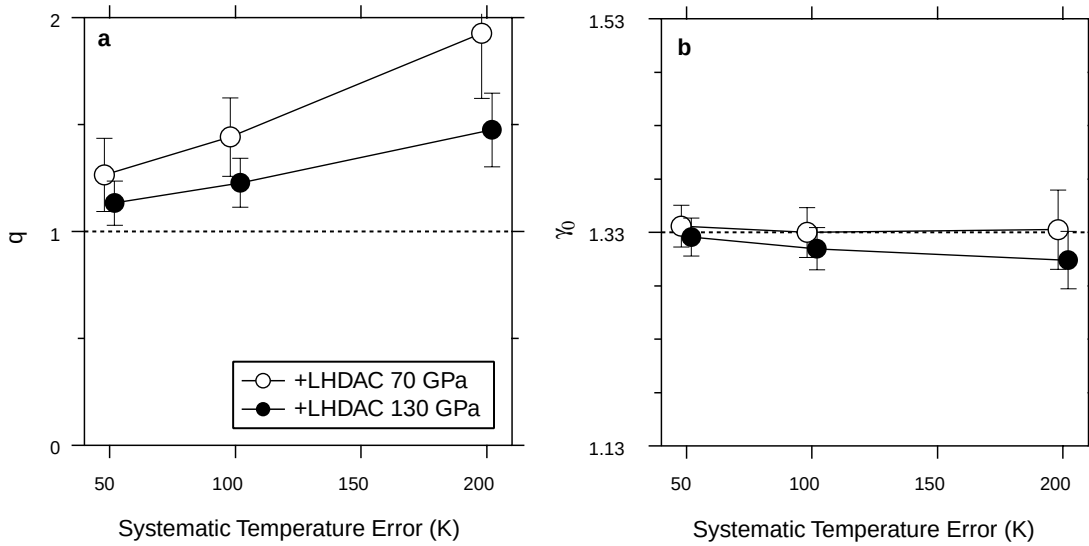

FIGURE 7. The fitted values of (**a**) q and (**b**) γ_0 vs. amount of systematic error added. The values used to generate the synthetic data are indicated as dashed lines. The symbols represent the average of fits to 100 data sets. The error bars are the standard deviation (1σ) of the fitted parameters of the 100 data sets. The points are slightly shifted from each other in order to prevent overlap of symbols.

systematic overestimation of q may be compensated to some extent by underestimation of γ_0 relative to the case for 70 GPa.

Currently available laser heating techniques yield an uncertainty of ~100 K (Fiquet et al. 1998). With this precision, by expanding the measured pressure range to 130 GPa, we can expect to obtain q and γ_0 with 1 standard deviation uncertainties of ±0.2 and ±0.03, respectively, assuming that we only have random errors on the temperature measurements. However, if there is also systematic error, we cannot eliminate the possibility of overestimation of q together with a slight underestimate of γ_0. However, γ_0 will still be reliable within the estimated uncertainty.

P-V-T EOS FIT FOR AVAILABLE DATA SETS

There have been several *P-V-T* measurements using the LVP (Wang et al. 1994; Utsumi et al. 1995; Funamori et al. 1996) which reached to as high as 29 GPa and 2000 K, corresponding to the uppermost part of the lower mantle. In addition, the thermal expansion parameter was measured at ambient pressure between 77 and 381 K (Ross and Hazen 1989). These data were fitted to the BMD equation by Jackson and Rigden (1996). In their study, they assumed $q = 1$ which enabled them to linearlize the BMD equation. They also obtained $\gamma_0 = 1.33(3)$ which is consistent with previous analyses (Wang et al. 1994; Anderson et al. 1996; Gillet et al. 1996).

As discussed above, we fit the data using the nonlinear least squares method. When q is fixed at 1, our results from fits to the lower pressure and temperature (LPT) data set agree with those of Jackson and Rigden (1996). It should be noted that the values of V_0 reported for the studies in the LPT data set varying between 162.2–162.6 Å^3. If, instead of using raw volume data, we normalized the volume by the V_0 value given for each study, we find that with q fixed at 1, we obtain slightly different results from Jackson and Rigden (1996), but they are consistent within the error range (Table 3). This normalized data set was used for all the fits below. When q is allowed to vary, the lower pressure and temperature data set was not able to constrain q reliably (Table 3), consistent with the simulation results discussed earlier.

Recently Fiquet et al. (1998) published *P,V,T* data at 30–60 GPa and 300–2500 K using the LHDAC. By itself, this data set is too small and covers too narrow of range to be reliably inverted. By combining this data with the LPT data (see Table 3), we obtain q = 2.7(5). This result is significantly different from the normal assumption of q = 1 which is the value consistent with 300K spectroscopic data (e.g., Lu and Hofmeister 1994).

Saxena et al. (1999) recently reported *P-V-T* measurements using their RHDAC system at 35–110 GPa and 300–1500 K. We also combined this data with the LPT data set. In this case, we obtained q = 1.7(3) and γ_0 = 1.40(4). γ_0 is consistent with earlier results (Table 3), but q is also significantly greater than 1 in this case.

Finally we also combined all available data sets and performed a fit. The result lies between the results using LPT+FI and LPT+SA alone (Table 3). Isotherms calculated from these parameters and selected data points are shown in Figure 8a. The difference between the solid lines and dashed lines is mainly caused by different q value (2.0 and 1.0, respectively). As temperature and pressure increase, the difference between the two isotherms are significant; at 100 GPa and 3000 K, the volume difference is 3%. At ambient conditions, using the result from LPT+FI+SA, we calculate the thermal expansion coefficient α_0 as $1.7(3) \times 10^{-5}$ K^{-1} and $(dK_T/dT)_P$ = –0.028(7) GPa/K. These are similar to those reported by Jackson and Rigden (1996) [α_0 = 1.57×10^{-5} K^{-1} and $(dK_T/dT)_P$ = –0.021 GPa/K]. However, the pressure dependence of these parameters, especially $(dK_T/dT)_P$ depends strongly on the value of q in the model. As shown in Figure 9, in the middle part of lower mantle, the thermal expansivity, α, and temperature dependence of isothermal bulk modulus, $(dK_T/dT)_P$, are different for the case of q = 1 and q = 2. However, as pressure increases, the difference between the two cases decreases. To better resolve these differences, further improvement in the data set are needed. The largest error source in determining $(dK_T/dT)_P$ is the uncertainty in q. The value of $(dK_T/dT)_P$ is important for comparing seismic bulk velocity profiles to laboratory data. The strong sensitivity of q and hence $(dK_T/dT)_P$ to systematic error in the reference isotherm and temperature measurement technique suggest that such

TABLE 3. Fitting results using various combinations of *P-V-T* data sets for $MgSiO_3$ perovskite

Data set	γ_0	q
LPT	1.35(2)	1*
	1.37(8)	1.2(1)
LPT + FI	1.48(5)	2.7(5)
LPT + SA	1.40(4)	1.7(3)
LPT + FI + SA	1.42(4)	2.0(3)
Stixrude et al. (1992) †	1.96(10)	2.5(17)
Jackson and Rigden (1996) ‡	1.33(3)	1*

Notes Other parameters were fixed at V_0 = 162.3 Å^3, K_{T0} = 261 GPa, K'_{T0} = 4.0, θ_0 = 1000 K. LPT = Lower pressure and temperature measurements (Ross and Hazen 1989; Wang et al. 1994; Utsumi et al. 1995; Funamori et al. 1996). These were also used by Jackson and Rigden (1996). FI = Fiquet et al. (1998). SA = Saxena et al. (1999).

* Fixed parameter

† V_0 = 163.13 Å^3, K_{T0} = 263(7) GPa, K'_{T0} = 3.9(4), and θ_0 = 1017(7) K for $(Mg,Fe)SiO_3$ perovskite.

‡ Fixed values of K_{T0} = 261 GPa, K'_{T0} = 4.0, q = 1, and θ_0 = 1000 K. However, they took K_{T0} as 262.4 GPa in their Table 5 based on Brillouin scattering measurements.

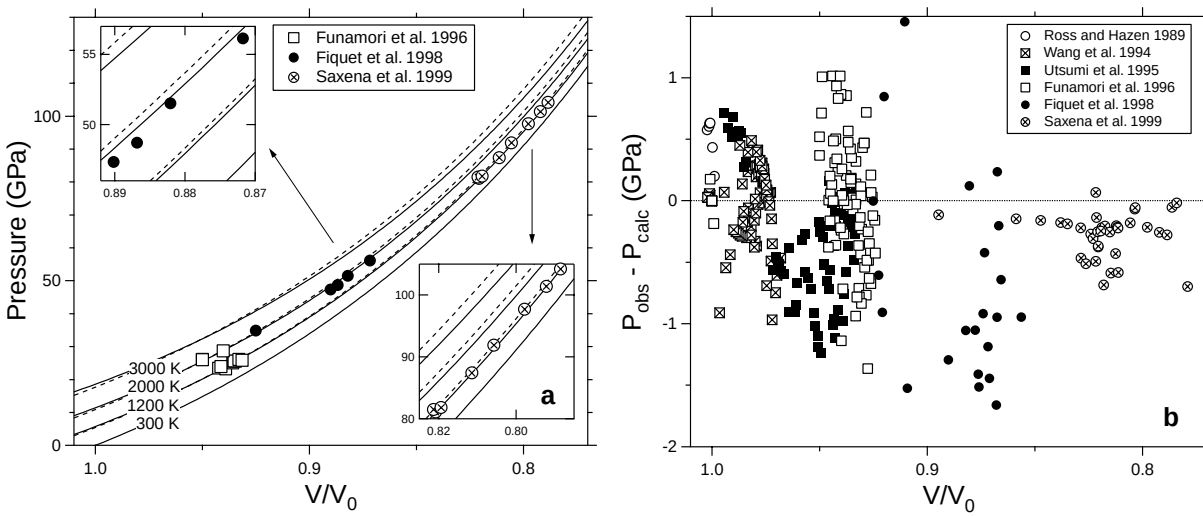

FIGURE 8. Equation of state fit to currently available data sets. (**a**) Isotherms for 300, 1200, 2000, and 3000 K for fits to LPT (dashed lines) and LPT+FI+SA (solid lines) data sets (see Table 3). Some of the measured data points at 1200 ± 100 K and 2000 ± 100 K are plotted for comparison. (**b**) The difference between the measured pressure and calculated pressure from fitted results for LPT data (q = 1) vs. volume. Estimated errors are smaller than symbol size for both plots.

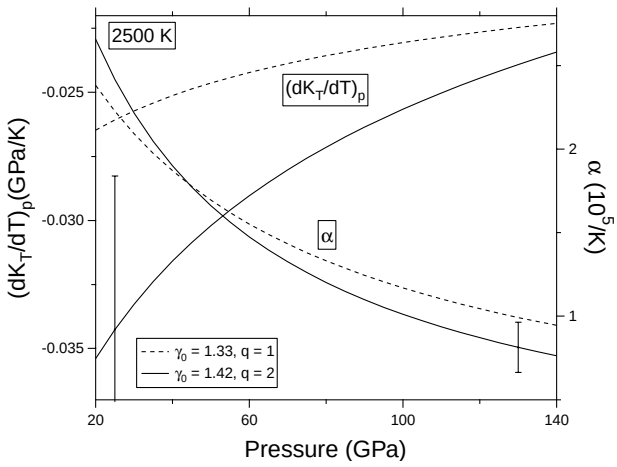

FIGURE 9. The variation of (**a**) $(dK_T/dT)_P$ and (**b**) α at 2500 K. Average estimated uncertainties are plotted.

comparisons should be performed with caution.

As shown in the inset of Figure 8a, isotherms calculated by the LPT+FI+SA fit are consistent with the measured data points, although some discrepancy remains in the case of Fiquet et al. (1998). The difference between the observed pressure and calculated pressure using the LPT model (q = 1) is shown as a function of volume compression in Figure 8b. The pressure residuals of the data of Wang et al. (1994) and Funamori et al. (1996) are randomly distributed. However, those of Utsumi et al. (1995), Fiquet et al. (1998), and Saxena et al. (1999) are systematically shifted to negative values. Since the data of Utsumi et al. (1995) lie between those of Wang et al. (1994) and Funamori et al. (1996), the effect of this systematic shift of Utsumi et al. (1995)'s data will be compensated. However, since all of the higher pressure data points show a systematic shift, they produce a difference in q values between the LPT fit and LPT+FI+SA fit.

Indeed, since we fixed all the parameters for P_{st} in Equation 1 as well as θ_0, only the variation of γ, and hence q, is important during the fitting. The negative shift in Figure 8b means the observed pressure is lower than the pressure from the LPT fit. If we include the FI and SA data sets in the fit, these data require a stronger change of pressure difference at given temperatures as volume increases. This means we must have a larger q.

However, the negative shift is much greater for the data points of Fiquet et al. (1998) than those of Saxena et al. (1999). This data set therefore results in the highest q (Table 3). Also the data points of Fiquet et al. (1998) show relatively large scatter (Fig. 8b). This systematic shift could be related to the different systematic error source of different techniques. As we discussed above, uncertainty in the reference (300 K) compression curve and systematic temperature overestimation could result in overestimation of q.

Although newly published high pressure and temperature data (Fiquet et al. 1998; Saxena et al. 1999) improve the resolution of q, there may remain systematic error sources which are technique dependent. As shown in Figure 8a, q is very sensitive to small changes of volume. Better constraints on q may be possible by performing experiments at 80–130 GPa and temperature above 2000 K.

The resolution of q for $MgSiO_3$ perovskite is also restricted by the limited range of thermal expansion parameter measurements at ambient pressure. Because of its abnormal behavior in the metastable field at high temperature and ambient pressure, reliable data is only available below room temperature (Ross and Hazen 1989; Wang et al. 1994). This results in uncertainties in the isotherms at low pressure and high temperature (Fig. 8a). q itself may also be volume dependent (Anderson et al. 1993) but the present data set is insufficient to resolve the volume dependence of this quantity.

All of these inversions were performed without weighting the data. Statistically it is reasonable to give a weight to each data point based on its estimated uncertainties. We also performed the fit by giving different weight to the data points from different techniques using the uncertainties given in Table 2. The uncertainties of volume and temperature were also included in weight using following equation.

$$\sigma_i^2 = \sigma^2(P_i) + \sigma^2(V_i)\left(\frac{\partial P}{\partial V}\right)_i^2 + \sigma^2(T_i)\left(\frac{\partial P}{\partial T}\right)_i^2 \qquad (7)$$

where σ is the estimated total uncertainty, σ(P), σ(V), and σ(T) are the uncertainties for P,V,T. The subscript i denotes individual data points. The derivatives are calculated using the equation derived from the BMD EOS.

By this method, the LPT data set has approximately four times more weight than FI data set and approximately three times more than SA data set. In this case, the result is mainly constrained by LPT data set; q = 1.3(10) for LPT+FI and q = 1.6(5) for LPT+SA and LPT+SA+FI. The fact that LPT has many more data points (250) than FI (27) or SA (37) also affects this result.

As discussed by Funamori et al. (1996), weighting will make the result most sensitive to ambient or lower pressure measurement rather than the high *P-T* measurement because of the inherently larger error of high *P-T* points. In this case, high *P-T* data points where $MgSiO_3$ perovskite is thermodynamically stable will have minimal effect on the fitted thermoelastic parameters. In addition, different groups may assign greatly different uncertainties to their data, despite using similar experimental techniques (Funamori et al. 1996). Thus we prefer the result from the analysis without weight.

The decrease of estimated uncertainties in fitted parameters by using experimental high *P-T* data agrees well with those obtained from simulation (cf., Table 3 and Fig. 5). For example, the estimated uncertainty of q for the LPT data set (±1.1) decreases by a factor of four if FI+SA are included. This was also observed in the synthetic data sets (LVP and LVP +LHDAC with 100 K temperature error and P_{max} = 130 GPa in Fig. 5a). However, the absolute uncertainty is about two times higher for the measured data sets. This could be due to either smaller errors assumed for the synthetic data compared with measured data or systematic difference in error source for different techniques.

ACKNOWLEDGMENTS

We thank Guoyin Shen for helpful discussions about the laser heating technique. Surendra Saxena kindly provided a preprint. Stas Sinogeikin and an anonymous reviewer provided us with valuable comments.

REFERENCES CITED

Akaogi, M. and Ito, E. (1993) Heat capacity of $MgSiO_3$ perovskite. Geophysical Research Letters, 20, 105–108.

Anderson, O.L. (1967) Equation for thermal expansivity in planetary interiors. Journal of Geophysical Research, 72, 3661–3668.

——(1998) Thermoelastic properties of $MgSiO_3$ perovskite using the Debye approach. American Mineralogist, 83, 23–35.

Anderson, O.L. and Masuda, K. (1994) A thermoelastic method for computing thermal expansivity, α, vs. T along isobars for silicate perovskite. Physics of the Earth and Planetary Interiors, 85, 227–236.

Anderson, O.L., Chopelas, A., and Boehler, R. (1990) Thermal expansivity versus pressure at constant temperature: a re-examination. Geophysical Research Letters, 17, 685–688.

Anderson, O.L., Oda, H., Chopelas, A., and Isaak, D.G. (1993) A thermodynamic theory of the Grüneisen ratio at extreme conditions: MgO as an example. Physics and Chemistry of Minerals, 19, 369–380.

Anderson, O.L., Masuda, K., and Guo, D. (1995) Pure silicate perovskite and the PREM lower mantle model: a thermodynamic analysis. Physics of the Earth and Planetary Interiors, 89, 35–49.

Anderson, O.L., Masuda, K., and Isaak, D.G. (1996) Limits on the value of δ_T and γ for $MgSiO_3$ perovskite. Physics of the Earth and Planetary Interiors, 98, 31–46.

Bina, C.R. (1995) Confidence limits for silicate perovskite equations of state. Physics and Chemistry of Minerals, 22, 375–382.

Fei, Y., Mao, H.-K., Shu, J., and Hu, J. (1992) *P-V-T* equation of state of magnesiowüstite $(Mg_{0.6}Fe_{0.4})O$. Physics and Chemistry of Minerals, 18, 416–422.

Fiquet, G., Andrault, D., Dewaele, A., Charpin, T., Kunz, M., and Häusermann, D. (1998) *P-V-T* equation of state of $MgSiO_3$ perovskite. Physics of the Earth and Planetary Interiors, 105, 21–31.

Funamori, N., Yagi, T., Utsumi, W., Kondo, T., and Uchida, T. (1996) Thermoelastic properties of $MgSiO_3$ perovskite determined by in situ X-ray observations up to 30 GPa and 2000 K. Journal of Geophysical Research, 101, 8257–8269.

Gillet, P., Guyot, F., and Wang, Y. (1996) Microscopic anharmonicity and equation of state of $MgSiO_3$-perovskite. Geophysical Research Letters, 23, 3043–3046.

Hemley, R.J., Stixrude, L., Fei, Y., and Mao, H.-K. (1992) Constraints on lower mantle composition from *P-V-T* measurements of $(Fe,Mg)SiO_3$-perovskite and (Fe,Mg)O. In Y. Syono and M. H. Manghnani, Ed., High-pressure research: application to earth and planetary sciences, pp. 183–189, Terra Scientific Publishing Company.

Hirose, K., Fei, Y., Ma, Y.Z., and Mao, H.-K. (1999) The fate of subducted basaltic crust in the Earth's lower mantle. Nature, 397, 53–56.

Jackson, I. (1998) Elasticity, composition and temperature of the Earth's lower mantle: a reappraisal. Geophysical Journal International, 134, 291–311.

Jackson, I. and Rigden, S.M. (1996) Analysis of *P-V-T* data: constraints on the thermoelastic properties of high-pressure minerals. Physics of the Earth and Planetary Interiors, 96, 85–112.

Kellogg, L.H., Hager, B.H., and van der Hilst, R.D. (1999) Compositional stratification in the deep mantle. Science, 283, 1881–1884.

Kesson, S.E., Gerald, J.D.F., and Shelley, J.M. (1998) Mineralogy and dynamics of a pyrolite lower mantle. Nature, 393, 252–255.

Knittle, E. and Jeanloz, R. (1987) Synthesis and equation of state of $(Mg,Fe)SiO_3$ perovskite to over 100 gigaphascals. Science, 235, 668–670.

Liu, L.-G. (1976) The high-pressure phases of $MgSiO_3$. Earth and Planetary Science Letters, 31, 200–208.

Lu, R. and Hofmeister, A.M. (1994) Thermodynamic properties of ferromagnesium silicate perovskites from vibrational spectroscopy. Journal of Geophysical Research, 99, 11785–11804.

Mao, H.-K., Hemley, R.J., Fei, Y., Shu, J.F., Chen, L.C., Jephcoat, A.P., and Wu, Y. (1991) Effect of pressure, temperature, and composition on lattice parameters and density of $(Fe,Mg)SiO_3$-perovskites to 30 GPa. Journal of Geophysical Research, 96, 8069–8079.

Press, W.H., Flannery, B.P., Teukolsky, S.A., and Wetterling, W.T. (1988) Numerical recipes in C - the art of scientific computing, 933 p. Cambridge University Press, U.S.A.

Ross, N. and Hazen, R.M. (1989) Single crystal X-ray diffraction study of $MgSiO_3$ perovskite from 77 to 400 K. Physics and Chemistry of Minerals, 16, 415–420.

Saxena, S.K., Dubrovinsky, L.S., Tutti, F., and Bihan, T.L. (1999) Equation of state of perovskite ($MgSiO_3$) based on experimentally measured data. American Mineralogist, 84, 226–232.

Shen, G. and Rivers, M.L. (1998) Experiments on deep Earth materials with a laser heated diamond cell at the APS. In Eos transactions, F864, American Geophysical Union.

Shim, S.-H., Duffy, T.S., and Shen, G. (1998) *P-V-T* equation of state of $MgSiO_3$ and $CaSiO_3$ perovskites to 60 GPa and 2000 K. In Eos transactions, F861, American Geophysical Union.

Stixrude, L., Hemley, R.J., Fei, Y., and Mao, H.-K. (1992) Thermoelasticity of silicate perovskite and magnesiowüstite and stratification of the Earth's mantle. Science, 257, 1099–1101.

Tomioka, N., and Fujino, K. (1997) Natural $(Mg,Fe)SiO_3$-ilmenite and -perovskite in the Tenham meteorite. Science, 277, 1084–1086.

Utsumi, W., Funamori, N., and Yagi, T. (1995) Thermal expansivity of $MgSiO_3$ perovskite under high pressures up to 20 GPa. Geophysical Research Letters, 22, 1005–1008.

van der Hilst, R.D. and Kárason, H. (1999) Compositional heterogeneity in the bottom 1000 kilometers of Earth's mantle: toward a hybrid convection model. Science, 283, 1885–1888.

van der Hilst, R.D., Widiyantoro, S., and Engdahl, E.R. (1997) Evidence for deep mantle circulation from global tomography. Nature, 386, 578–584.

Wang, Y., Weidner, D.J., Liebermann, R.C., and Zhao, Y. (1994) *P-V-T* equation of state of $(Mg,Fe)SiO_3$ perovskite: constraints on composition of the lower mantle. Physics of the Earth and Planetary Interiors, 83, 13–40.

Williams, Q., Revenaugh, J., and Garnero, E. (1998) A correlation between ultra-low basal velocities in the mantle and hot spot. Science, 280, 546–549.

Yeganeh-Haeri, A. (1994) Synthesis and re-investigation of the elastic properties of single-crystal magnesium silicate perovskite. Physics of the Earth and Planetary Interiors, 87, 111–121.

MANUSCRIPT RECEIVED APRIL 5, 1999
MANUSCRIPT ACCEPTED OCTOBER 13, 1999
PAPER HANDLED BY ROBERT C. LIEBERMANN